Shape Optimal Design on Constrained Single-chamber Mufflers by Gradient Method

Tian-Syung Lan[*]

Ying-Chun Chang[**], **Long-Jyi Yeh**[**], ***and***
Min-Chie Chiu[**]

[*]Department of Mechanical Engineering
De Lin Institute of Technology
Tuchen, Taiwan 236, R.O.C.

[**]Department of Mechanical Engineering
Tatung University
Taipei, Taiwan 10451, R.O.C.

ABSTRACT

The constraint problem in muffler is often occurred in practical engineering work for the demand of maintenance and operation. However, the study in enhancing the acoustic performance of muffler under space constraints is still rarely accomplished. Therefore, the shape optimization to maximize the acoustic performance of mufflers becomes an essential issue, accordingly.

The shape optimization of single-chamber mufflers is fully derived and discussed in this paper by using four-pole transfer method [1,2,3,4] and several powerful gradient methods, including exterior penalty function method (EPFM), interior penalty function method (IPFM) and feasible direction method (FDM) [5,6]. To avoid the solution being trapped in a local maximum, a global searching technique of initial design data by graphic analysis on sensitivity [7] is then adopted. Thereafter, the successive optimal algorithm of gradient searching techniques based on the initial design data is then carried out individually. Before optimization, one example is tested and compared with the experiment data [8] for accuracy check of mathematical model. In addition, a numerical case of noise elimination on pure tone noise inside a building is exemplified for the shape optimization. Consequently, these optimal results are confirmed by Kuhn-Tucker Condition for the accuracy purpose. It is shown that the accuracy in mathematical model and the convergence in numerical optimization are acceptable. The shape optimization on the single-chamber muffler design proposed in this study surely provides a quick and economical procedure under space limitations without redundant testing.

Key Words：four-pole matrix 、shape optimization、mathematical gradient method、single-chamber muffler、space constraints

以數學梯度法進行限制尺寸下的單腔消音器之外型最佳化設計

藍天雄*
張英俊** 葉隆吉** 邱銘杰**

*德霖技術學院 機械工程系
E-mail: ycchang@ttu.edu.tw

**大同大學 機械工程系

摘要

在實務工程設計裡，由於維修及操作的需要，往往會侷限消音器的設計空間，然而至目前為止，鮮少有相關文獻探討”在限制尺寸下強化音響性能”的研究，因此，以外型最佳化來極大化消音器的音響性能，便成了一個重要的研究主題。

以四埠傳輸矩陣[1,2,3,4]結合功能強大的梯度法，包括圈外罰則函數法(EPFM)、圈內罰則函數法(IPFM)及可行進方向法(FDM)等三數值方法[5,6]，進行”單腔消音器在限制空間下的外型最佳化”，將在本文中被充分推演與討論；為了避免在最佳化數值搜尋中，陷入局部最大值解的泥沼裡，以”圖形系統之靈敏度分析”進行全域式的初始值搜尋技巧[7]因此被應用於本文內，此後，再依據此初始設計值分別進行後續三項數值梯度的最佳化搜尋，在進行最佳化之前，為了驗證數學模式的準確度，將進行一個簡例計算並與實驗值[8]做比較，此外，本文將以一個廠房內的單頻音處理做為外型最佳化的數值討論範例，三種最佳化搜尋的成果，將以 Kuhn-Tucker Condition 來驗證其精確度，最後之結果證明，不論是數學模式的準確度或是數值最佳化的收斂性均是可被接受的。本文在限制尺寸下的單腔消音器的外型最佳化研究上，確實可提供一快速且經濟的方法，以避免傳統冗長的測試。

關鍵詞：4 埠矩陣、外型最佳化設計、數學梯度法、單腔消音器、限制空間

1. NOMENCLATURE

C_o : sound speed (m s^{-1})
D : diameter (m)
$F(\overline{X})$: unmodified objective function
f : cyclic frequency
$g_i(\overline{X})$: the i-th inequality constraints
j : $\sqrt{-1}$
k : wave number.
L : length (m)
M_i : mean flow Mach number at i
P : total flow pressure (Pa)
p_i : pressure; acoustic pressure at i (Pa)
$R(\overline{X})$: residual vector
r_p : penalty factor
r_p' : penalty factor
S_i : section area at i (m^2)
STL : sound transmission loss (dB)
U_i : acoustic volume velocity at i (m^3 s^{-1})
u_i : acoustic particle velocity at i (m s^{-1})
V : total flow velocity (m s^{-1})
V_i : mean flow velocity at i (m s^{-1})
$\overline{X}$: design parameter set
ρ_o : air density (kg m^{-3})
Φ : modified objective function
ϕ : potential function in acoustic flow
λ_j : the j-th vector of Lagrange multiplier
$\nabla F(\overline{X})$: function gradient vector

2. INTRODUCTION

Nowadays, a variety of products with low-noise have become more and more competitive in sales and profit [9]. As reported by America Petroleum Institute (API) [10], it shows that reactive silencer (muffler) is particularly suited to low frequency noise cancellation. Whilst most of the electric machine radiate low frequencies [11], the muffler system is thus habitually adopted in the noise reduction. However, the shape of muffler is often confined for the necessity of maintenance and operation. Even that many researches of mufflers were well developed, the performance maximization of muffler under space constraints is still rarely accomplished. Therefore, the interest to optimize STL of the muffler under space constraints is arising in the field of acoustics.

A numerical case of single-chamber mufflers is also fully illustrated in this paper. To achieve the shape optimization in muffler design, the mathematical gradient methods are in conjunction with four-pole matrix method of which the plane wave theorem is assumed

[1,2,3,4].

3. THEORETICAL BACKGROUND

In this paper, the single-chamber muffler with simple expansion and contraction is discussed and depicted in Fig.1. For the ease

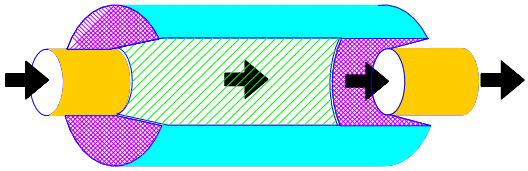

Fig.1. 3-D single-chamber muffler

of theoretical derivation on mufflers, two kinds of muffler components, including (1) straight duct and (2) simple expansion/contraction duct, are firstly identified. On the basis of plane wave theorem, a transfer matrix between inlet and outlet can then be deduced in each muffler element. By the combination of transfer matrix for all muffler elements, the complete four-pole matrix of the whole muffler can be built. Furthermore, the STL can be easily calculated by means of the four-pole matrix. By the classification of distinct component in muffler, three elements of straight ducts and two elements of simple expansion/contraction ducts are distinguished. The muffler's flowing condition and location is specified in Fig.2, where the whole flow condition within the muffler can be presented by six nodes (pt1~pt6) that are chosen within each elements individually. The theoretical derivation for each element is illustrated as follows:

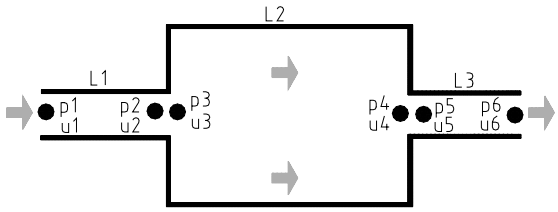

Fig.2. Flow condition of a single-chamber muffler

1. Straight Duct [1, 2, 3, 4]

With the momentum equation where the body force and viscosity effects are ignored, the Navier-Stokes equation is then simplified as

$$\rho[\partial V/\partial t + V.\nabla V] = -\nabla P \qquad (1)$$

Developing V, ρ, and P; Eq. (1) is rearranged as

$$\nabla[\rho_o(\partial\phi/\partial t + V_o\partial\phi/\partial x) - p] = 0 \qquad (2)$$

The analytical solution for the 1-D partial differential Eq. (2) is then deduced and obtained as

$$p = jw\rho_o\phi + \rho_o V_o\partial\phi/\partial x; \qquad (3)a$$

where $\phi = [Ae^{-jk_1x} + Be^{+jk_2x}]e^{j\varpi t}$; $k_1 = k/(1+M)$; $k_2 = k/(1-M)$; (3)b

Finally, the four-pole matrix between point 1 and point 2 with mean flow is shown in Eq. (4).

$$\begin{pmatrix} p_1 \\ \rho_o c_o u_1 \end{pmatrix} = e^{-jM_1kL_1/(1-M_1^2)} \begin{bmatrix} b11 & b12 \\ b21 & b22 \end{bmatrix} \begin{pmatrix} p_2 \\ \rho_o c_o u_2 \end{pmatrix} \qquad (4)a$$

where

$$\begin{cases} b11 = \cos(\frac{kL_1}{1-M_1^2}) \\ b12 = j\sin(\frac{kL_1}{1-M_1^2}) \\ b21 = j\sin(\frac{kL_1}{1-M_1^2}) \\ b22 = \cos(\frac{kL_1}{1-M_1^2}) \end{cases} \quad (4)b$$

As the derivation in Eq. (4), the four-pole matrix between point 3 and point 4 with mean flow is expressed in Eq. (5).

$$\begin{pmatrix} p_3 \\ \rho_o c_o u_3 \end{pmatrix} = e^{-jM_2 kL_2/(1-M_2^2)} \begin{bmatrix} c11 & c12 \\ c21 & c22 \end{bmatrix} \begin{pmatrix} p_4 \\ \rho_o c_o u_4 \end{pmatrix} \quad (5)a$$

where

$$\begin{cases} c11 = \cos(\frac{kL_2}{1-M_2^2}) \\ c12 = j\sin(\frac{kL_2}{1-M_2^2}) \\ c21 = j\sin(\frac{kL_2}{1-M_2^2}) \\ c22 = \cos(\frac{kL_2}{1-M_2^2}) \end{cases} \quad (5)b$$

Thus, the four-pole matrix between point 5 and point 6 with mean flow is expressed in Eq. (6).

$$\begin{pmatrix} p_5 \\ \rho_o c_o u_5 \end{pmatrix} = e^{-jM_3 kL_3/(1-M_3^2)} \begin{bmatrix} d11 & d12 \\ d21 & d22 \end{bmatrix} \begin{pmatrix} p_6 \\ \rho_o c_o u_6 \end{pmatrix} \quad (6)a$$

where

$$\begin{cases} d11 = \cos(\frac{kL_3}{1-M_3^2}) \\ d12 = j\sin(\frac{kL_3}{1-M_3^2}) \\ d21 = j\sin(\frac{kL_3}{1-M_3^2}) \\ d22 = \cos(\frac{kL_3}{1-M_3^2}) \end{cases} \quad (6)b$$

2. Expansion/Contraction Duct [4]

As derived by Munjal [4], both of the identity of pressure and the continuity of volume flow between point 2 and point 3 with mean flow is expressed in Eq. (7).

$$p_2 = p_3; U_2 = U_3 \quad (7)$$

By substituting particle velocity u into continuity Eq. (7), the transfer matrix for Eq. (7) is thus

illustrated as

$$\begin{pmatrix} p_2 \\ \rho_o c_o u_2 \end{pmatrix} = \begin{bmatrix} 1 & 0 \\ 0 & \frac{S_3}{S_2} \end{bmatrix} \begin{pmatrix} p_3 \\ \rho_o c_o u_3 \end{pmatrix} \qquad (8)$$

As the derivation of Eq. (8), the transfer matrix between pt4 and pt5 is expressed as

$$\begin{pmatrix} p_4 \\ \rho_o c_o u_5 \end{pmatrix} = \begin{bmatrix} 1 & 0 \\ 0 & \frac{S_5}{S_4} \end{bmatrix} \begin{pmatrix} p_5 \\ \rho_o c_o u_5 \end{pmatrix} \qquad (9)$$

3. Combination of System Matrix

Using the matrix substitution on Eqs. (4)~(6), (8), and (9), one has

$$\begin{pmatrix} p_1 \\ \rho_o c_o u_1 \end{pmatrix} = \begin{bmatrix} T11 & T12 \\ T21 & T22 \end{bmatrix} \begin{Bmatrix} p_6 \\ \rho_o c_o u_6 \end{Bmatrix} \qquad (10)$$

The sound transmission loss (STL) [4] of a muffler is defined as

$$STL(f, Q, L_1, L_2, L_3, D_1, D_o, D_2) = 20\log\left(\frac{|T11 + T12 + T21 + T22|}{2}\right) + 10\log\left(\frac{S_1}{S_3}\right) \qquad (11)\text{a}$$

where $Q = V_i S_i$; $V_i = M_i c_o$; $f = \frac{kc_o}{2\pi}$; $L_3 = L_o - L_1 - L_2$ (11)b

4. CASE STUDY

A noise control of a venting noise emitted from pipe outlet, which is with 0.0762 m (commercial standard pipe dimension) in diameter, is introduced as the numerical case. It is found that the pure tone effect occurred at 500Hz is remarkable. In addition, the available space for silencer inside the building is specified as 0.5^{M}L*0.5 ^{M}W *3.0^{M}H.. To reduce the sound energy at 500Hz, an attempt for optimal design on mufflers is then made under the boundary constraint. Both the graphic analysis and numerical assessments are carried out as follows. The space constraint for muffler is shown in Fig.3, and the design volume flow rate is confined to 0.8CMS

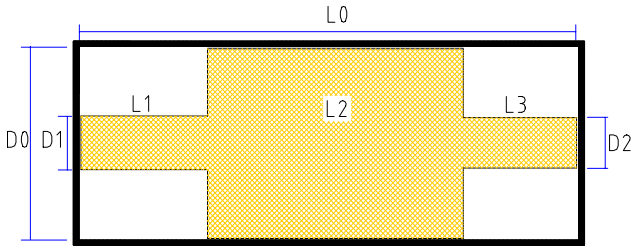

Fig.3. Space constraints of a single-chamber muffler [Lo=3.0m ; Do=0.5m]

5. MODEL CHECK

Before performing the optimal simulation on mufflers, the accuracy check of mathematical model on muffler is made by experiment data [8]. As depicted in Fig.4, the accuracy comparisons between theoretical and experiment data for the model proves that they are in good agreements. Therefore, the proposed fundamental mathematical model is

valid under the cutoff frequency of $f = 3.83c/\pi D$ in which D is the diameter of muffler.

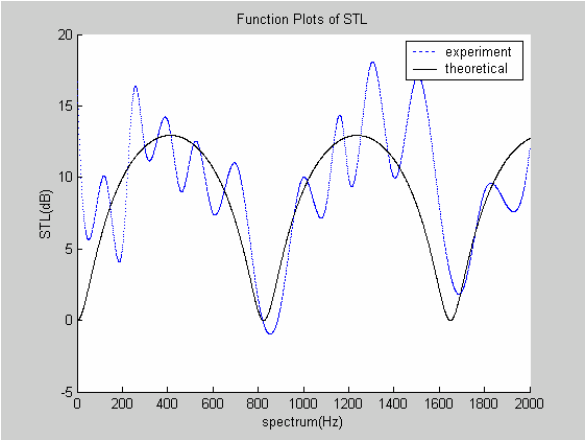

Fig.4. Performance of a single-chamber muffler at the mean flow velocity of 3.4m/sec[D_1=D_2=0.0365 (m);Do=0.108(m);L_1=L_3=0.1(m);L_2=0.208(m)]

Consequently, the models linked with numerical method are applied for the shape optimization as following paragraph.

GRAPHIC ANALYSIS ON SENSITIVITY

1. Sensitivity Analysis

On the basis of fixed values in *f* (500Hz), *Lo*(3.0m), *Do*(0.5m), *Q*(0.8CMS) and $L_3(Lo-L_1-L_2)$, the effective design parameters are simplified as L_1,L_2, $D_1$and D_2.

The graphic analysis on sensitivity with respect to these parameters are also discussed as below:

(1) L_1 and L_2 Effects

STL with respect to design parameters L_1 and L_2 at 500Hz is shown in Fig.5, which reveals that *STL* will be changed by varying either L_1 or L_2. As indicated in Fig.5, the periodic curve of *STL* with respect to variable L_2 is found. Obviously, the sensitivity of L_2 is stronger than that of L_1.

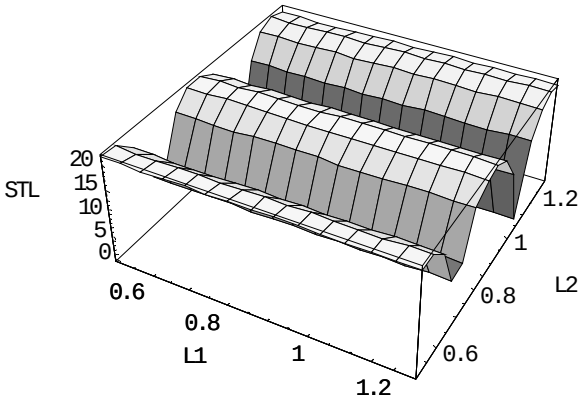

Fig.5. *STL* with respect to L_1 and L_2

(2)L_1 and D_1 Effects

The relationship between *STL*, D_1 and L_1 at 500 Hz is graphed in Fig.6. As illustrated in Fig.6, *STL* will be varied as a convex when D_2 is increased. However, the variety of *STL* with respect to L_1 is inert. Obviously, the sensitivity of D_2 is higher than that of L_1.

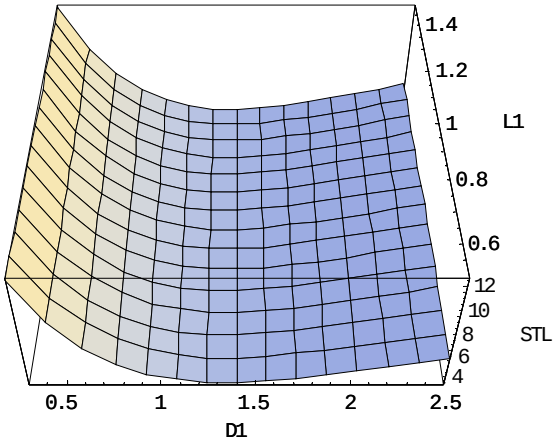

Fig.6. *STL* with respect to L_1 and D_1

(3) L_1 and D_2 Effects

As shown in Fig.7, the *STL* with respect to design parameters D_2 at 500Hz is behaved as a convex, too. Conversely, the variety of *STL* to L_1 is rare. Unquestionably, D_2 is more sensitive than L_1.

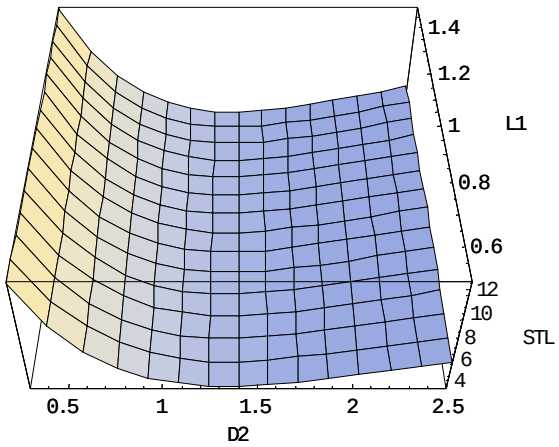

Fig.7. *STL* with respect to L_1 and D_2

(4) D_1 and D_2 Effects

By varying D_1 and D_2 simultaneously, the variety of *STL* at 500Hz is shown in Fig.8, Observably, *STL* will be increased either D_1 or D_2 being decreased. Without doubt, both of D_1 and D_2 are sensitive concurrently.

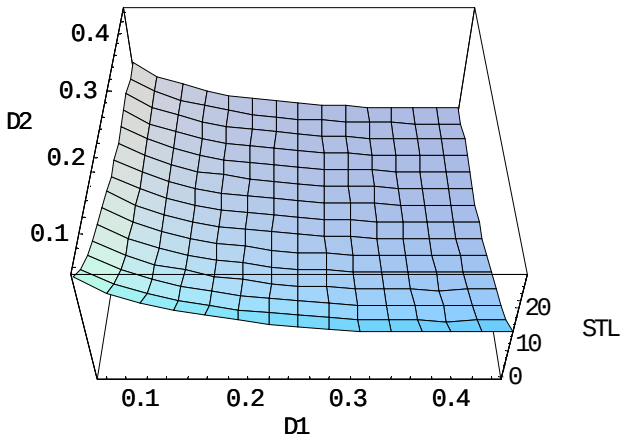

Fig.8. *STL* with respect to D_1 and D_2

(5) L_2 and D_1 Effects

The response of *STL* with respect to L_2 and D_1 at 500Hz is plotted in Fig.9. As revealed in Fig.9, the periodic variety to L_2 and the inversely decreased curve to D_2 are demonstrated. Both of L_2 and D_1 are the effective design parameter L_2 to *STL*.

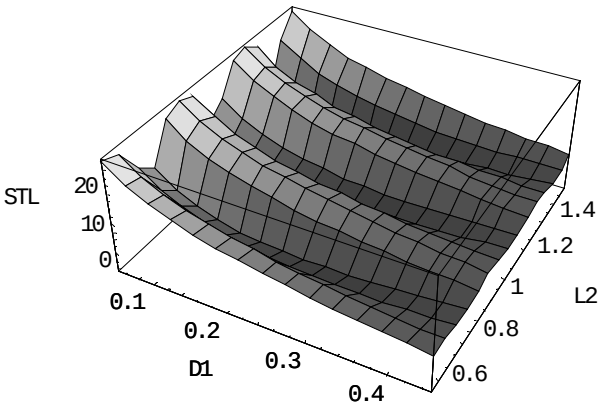

Fig.9. *STL* with respect to L_2 and D_1

(6) L_2 and D_2 Effects

As shown in Fig.10, the variety of *STL* with respect to L_2 at 500Hz is in a periodic form.

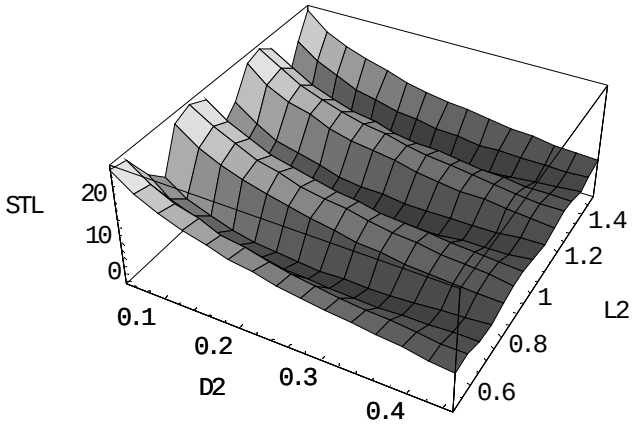

Fig.10. STL with respect to L2 and D2

Moreover, STL will be increased when D2 becomes small. Visibly, both of L2 and D2 are have the high sensitivity to *STL*.

2. Discussion of Sensitivity

According to Figures 6~10, it is obvious that D_1 & D_2 & L_2 are the effective parameters with higher sensitivity in *STL*. Besides, at the condition of D_1 < 1.5 (m) and D_2 < 1.5 (m), *STL* will be increased when either D_1 or D_2 is decreased.

To avoid the extra pressure drop and unexpected second noise induced by high speed flow [12], the design data of D_1 & D_2 are thus defined to be not less than 0.0762 (m), the diameter of existed pipe outlet. Therefore, the values of D_1 and D_2 are set to 0.0762 (m) simultaneously. From the prediction of computer graphic system, three peak values of *STL* at 500Hz are occurred when L_2 is in 0.5m, 0.8m, and 1.2m. Therefore, three sets of initial design data are found and described as follows.

That is (a) L_1=1.25 , L_2=0.5; (b) L_1=1.25 , L_2=0.8 ; and (c) L_1=1.25, L_2=1.2. The first set of the above design data is chosen as the initial design data for the succeeding optimal numerical assessment.

NUMERICAL OPTIMAL ASSESSMENT

According to the sensitivity analysis in above discussion, the four kind of design parameter (L_1, L_2, D_1, D_2) are reduced to two (L_1, L_2). For the availability in muffler's manufacture, an assumption is made that the minimal length of each segment of pipe are not less than 0.1 (m). To maximize the value of *STL*, the minimal value of $-STL(L_1, L_2)$ is planned and proceeded as below.

1. Mathematical Formulation [5]

Minimize $F(\overline{X}) = -STL(L_1, L_2)$

, Objective function

Subjected to $g_j(\overline{X}) \le 0 \quad j = 1,3$ inequality constraints

where $\overline{X} = \begin{bmatrix} X_1 \\ X_2 \end{bmatrix} = \begin{bmatrix} L_1 \\ L_2 \end{bmatrix}$ design variable

the shape constraints are $L_1 \ge 0.1$; $L_2 \ge 0.1$; $L_3 = Lo - L_1 - L_2 \ge 0.1$

The initial design data is $(X_1, X_2)_{Starting\_pt.} = (1.25, 0.5)$. To reach the numerical design data, three kinds of search algorithms used in the optimal design process are carried out and briefly introduced as follows.

(1) Exterior Penalty Function Method [5]

By using exterior penalty function method (EPFM), Φ is defined as

$$\Phi(\overline{X}, r_p) = F(\overline{X}) + r_p.P(\overline{X}) = F(\overline{X}) + r_p \sum_{i=1}^{3} \{\max[0, g_i(\overline{X})]\}^2$$

where $g_1(\overline{X}) = 0.1 - X_1; g_2(\overline{X}) = 0.1 - X_2;$

$g_3(\overline{X}) = X_1 + X_2 - 2.9$

(2)Interior Penalty Function Method [5]

By using interior penalty function method (IPFM), Φ is defined as

$$\Phi(\overline{X}, r_p', r_p) = F(\overline{X}) + r_p' \sum_{j=1}^{3} \frac{-1}{g_j(\overline{X})}$$

where $g_1(\overline{X}) = 0.1 - X_1; g_2(\overline{X}) = 0.1 - X_2; g_3(\overline{X}) = X_1 + X_2 - 2.9$

(3)Feasible Direction Method [5]

The feasible direction method (FDM) proceeds from one constraint to another in a zig-zag manner until the optimum is located. A tendency of this method is to zig-zag between the constraints.

2. Iteration and Results

Taking the initial design data as first trial value, a successive iteration together with the search algorithms, such as interior penalty function method, exterior penalty function method, and method of feasible direction are to be carried out individually.

The results of numerical assessment with three search techniques are shown in Table 1.

Table 1 Results of numerical assessments in three kinds of search technique

Iter.	EPFM		IPFM		FDM	
No	L_1	L_2	L_1	L_2	L_1	L_2
0	1.25	0.5	1.25	0.5	1.25	0.5
1	1.25	0.5146	1.2499	0.5181	1.1	0.9
2	1.25	0.5146	1.2499	0.5150	1.1	1.0
3			1.2499	0.5140	1.1	0.8554
4			1.2499	0.5137	1.1	0.8582
7			1.2499	0.5136	1.099	0.7579
10			1.25	0.5613	1.099	0.8454
13			1.25	1.1629	1.1	0.8547
16			1.25	1.2011	1.1	0.8575
19			1.25	1.20111	1.1	0.8579

The optimal *STL* with respect to the optimal design parameters in three methods are shown in Table 2. The three sets of design data are $\overline{X}_1 = \begin{bmatrix} 1.25 \\ 0.50001 \end{bmatrix}$; $\overline{X}_2 = \begin{bmatrix} 1.25 \\ 1.19798 \end{bmatrix}$; and $\overline{X}_3 = \begin{bmatrix} 1.1 \\ 0.85791 \end{bmatrix}$

The optimal STL with respect to the optimal design parameters in three methods are shown in Table 2.

Table 2 Optimal STL with respect to the optimal design parameters in three methods

Method	L_1	L_2	*STL*
EPFM	1.25	0.5146	26.6647
IPFM	1.2499	1.2011	26.6642
FDM	1.1	0.8579	26.6647

According to Table 2, it is observed that both the first and third design data have the better *STL* of 26.664dB at the respective design data. By using the third set of design data, which results in the higher value of *STL*, the profile of *STL* with respect to frequency domain is illustrated in Fig.11.

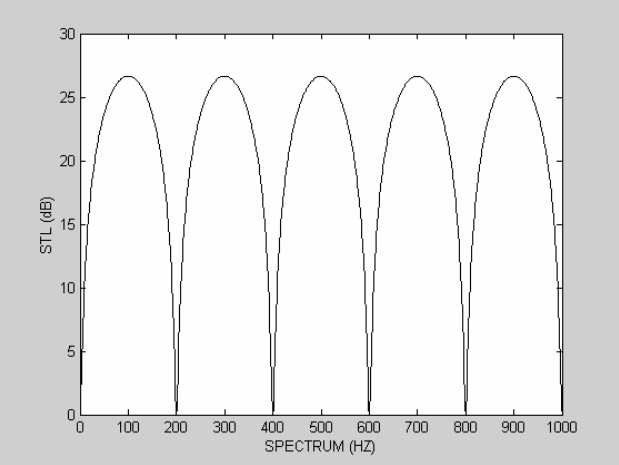

Fig.11. *STL* with respect to frequency

3. Accuracy

The Kuhn-Tucker's necessary conditions are then applied for the check of convergence criterion in each optimal approach [5]. The Kuhn-Tucker Condition is described as follows:

$$\lambda_j g_j(\overline{X}) = 0 \qquad j = 1,3 \qquad \lambda_j \geq 0$$

$$R(\overline{X}) = \nabla F(\overline{X}) + \sum_{j=1}^{3} \lambda_j \nabla g_j(\overline{X})$$

and

$$g_1(\overline{X}) = 0.1 - X_1; g_2(\overline{X}) = 0.1 - X_2; g_3(\overline{X}) = X_1 + X_2 - 2.9$$

where λ_j, $\nabla F(\overline{X})$ and $R(\overline{X})$ represent vector of Lagrange multiplier, function gradient vector and residual vector, respectively. To meet the converge criterion, the conditions of "$R(\overline{X}) \approx 0$" and "$\lambda_j \geq 0$" are required. By taking $\overline{X}_1$, $\overline{X}_2$ and $\overline{X}_3$ into Kuhn-Tucker Condition's checking process, the results are shown in Table 3 which reveals that the third set of design data, $\overline{X}_3$, will more meet Kuhn-Tucker Condition where the respective Lagrange

Multipliers are positive and the residual vectors are closed to zero.

Table 3 Results of Kuhn-Tucker Condition's checking process in three methods

Method	**Lagrange Multipliers**			**Residual Vector**	
	λ_1	λ_2	λ_3	$\{R_1\}$	$\{R_2\}$
EPFM	-1.01	0.79	-1.01	0.59E-07	-0.12E-06
IPFM	0.0	0.0	-1.06	-1.06644	-9,12E-06
FDM	2.69	5.79	2.69	-.12E-06	-.24E-06

On the whole, the optimal values obtained by three kinds of optimal searching techniques are very closed for each other.

CONCLUSIONS

The maximal noise reduction under space constraints is very important and essential to the design of muffler. Based on one dimensional plane wave theory, the theoretical STL of single-chamber mufflers is deduced by the four-pole transfer matrix in this paper. The proposed fundamental mathematical model in design frequency of 500 Hz is surely in validity of which the frequency domain should be less than the cutoff frequency of $f = 3.83c/\pi D$ (i.e. 837 Hz). In addition, the theoretical model is verified accurate by experimental data before optimization. Besides, our proposed computer's graphic system presents quick examination of all the global peak points and the resolutions of sensitivity analysis for every individual design parameter. According to the developed graphic analysis on sensitivity, initial design data is thus primarily determined. Using the fundamental data as initial design value, three kinds of searching techniques are then processed. Therefore, much accurate solutions can furthermore be achieved. The Kuhn-Tucker Condition is then applied to verify the accuracy of the solution. This study offers a quick way to not only organize the best drawing in muffler but also compromise the effectiveness for the constrain task which is usually occurred in enclosed building. Through the case study, it is found that the optimal design of single-chamber mufflers for the sound transmission loss at 500Hz is accurate through the confirmation of Kuhn-Tucker Condition.

REFERENCES

1. Prasad, M. G., A note on acoustic plane waves in a uniform pipe with mean flow, Journal of Sound and Vibration, 95(2), 284-290 (1984).
2. Munjal, M. L., Prasad, M. G., Transfer matrix of a uniform tube with moving medium and linear temperature gradient., J. Acoust. Soc. Am., 80(50), 1501-1506 (1986).
3. Prasad, M. G., Crocker, M. J., Studies of acoustical performance of a multi-cylinder engine exhaust muffler system, Journal of Sound and Vibration, 90(4), 491-508 (1983).
4. Munjal, M. L., Acoustics of ducts and mufflers with application to exhaust and ventilation system design, John Wiley & Sons, New York (1987).
5. Vanderplaats, Garret N., Numerical optimization techniques for engineering design : with applications, McGraw-Hill , New York (1984).
6. Weeber, K. , Ratnajeevan S., Hoole H., Geometric parametrization and constrained optimization techniques in the design of salient pole synchronous machines, IEEE Transaction on Magnetics, 28(4), 1948-1960 (1992).
7. Yeh, L. J., Chiu, M. C., Lay, G. J. Computer aided design on single expansion muffler under space constraints. Proceedings of the 19th National Conference on Mechanical Engineering (The Chinese Society of Mechanical Engineers), C7: pp.625-633, Yun Lin, R.O.C., 2002.
8. Wang, C. N., Hsieh, C. C., Experimental study for muffler components with flow, Bulletin of the College of Engineering, N.T.U., No.78, 67~74 (2000).
9. Kaiser, L., Bernhardt, H., Noise control on computer and business equipment using speed control blowers, IEEE, (2), 114-117 (1989).
10. Tracor Inc., Guidelines on noise, American Petroleum Institute (1973).
11. Timar, P. L., Noise and vibration of electrical machines, Elsevier Science , New York (1989).
12. Schaffer,Mark E., A practical guide to noise and vibration control for HVAC systems, ASHRAE (1991).